JOURNAL OF MATERIALS SCIENCE 25 (1990) 2039–2046

Thickness effects in microlayer composites of polycarbonate and poly(styrene–acrylonitrile)

M. MA*, K. VIJAYAN†, A. HILTNER, E. BAER
Center for Applied Polymer Research, and Department of Macromolecular Science, Case Western Reserve University, Cleveland, Ohio 44106, USA

J. IM
The Dow Chemical Company, Midland, Michigan 48674, USA

Coextruded microlayer sheet consisting of alternating layers of polycarbonate (PC) and styrene–acrylonitrile copolymer (SAN) exhibits improved properties such as toughness and ductility as the number of layers is increased. In this study, the composition was kept essentially constant, as was the sheet thickness at 1.2 mm, and the layer thickness was changed by varying the total number of layers from 49 to 776. All the compositions exhibited macroscopic yielding in uniaxial tension but the fracture strain, which represents neck propagation, increased with the number of layers. The increased ductility was attributed to a transition in the microdeformation behaviour observed when microspecimens were stretched in the optical microscope. When the layers were thicker, individual layers exhibited behaviour characteristic of the bulk, that is SAN crazed or cracked while shear bands initiated in PC from the craze tips. As the layer thickness decreased, crazing or cracking of the SAN was suppressed and shear bands that extended through several layers produced shear yielding of both PC and SAN. Calculations showed that when the layer thickness is sufficiently small, impingement of a PC shear band on the interface creates a local shear stress concentration. As a result the shear band continues to grow through the SAN layer and subsequently, at the point of instability, shear yielding can occur in both PC and SAN layers.

1. Introduction

Microlayer coextrusion is an advanced coextrusion process [1, 2]; it differs from the conventional multilayer coextrusion in that many more layers, usually more than 50 but sometimes as many as several thousand, are produced in one extrusion step. Two or three polymers can be incorporated in various arrangements, the most common are ABABAB... and ABCBABCB.... Total thickness as well as layer thickness can be controlled, and in the case of thin films, the individual layer thickness may be reduced to a few tens of nanometres.

Unique properties of the microlayer structures have been reported. For example, films exhibiting colourful irridescence were produced by alternating two polymers of different refractive indices, such as polypropylene and polystyrene or polycarbonate and polymethylmethacrylate, and approximately controlling the volume fraction and layer thickness [3, 4]. Films which reflect ultraviolet or near infrared radiation have been obtained by microlayer coextrusion [5]. Water-barrier properties of 125-layer polyethylene/polystyrene films were not affected significantly by crumpling, presumably because the cracks or flaws in the polystyrene were randomized [6]. In the same paper, mutual reinforcement was observed in biaxially oriented microlayer films of polypropylene and polystyrene over a wide range of composition ratios.

Recently, a study of thick microlayer sheet has been undertaken in which polycarbonate (PC), a tough polymer, is combined with styrene–acrylonitrile copolymer (SAN), a brittle material which exhibits excellent interfacial adhesion to polycarbonate [7]. Not surprisingly, the tensile and impact properties showed a brittle-to-ductile transition when the PC/SAN volume ratio was increased but the overall thickness was maintained at about 1.2 mm. However, when the layer thickness was decreased by increasing the number of layers from 49 to 766 while maintaining the sheet thickness constant, mechanical properties such as ductility and toughness were improved for any PC/SAN ratio.

Microdeformation studies of the 49-layer composite showed that the initial irreversible deformation event was crazing or cracking of the SAN layers followed by initiation of microshear bands in the PC layers at the craze tips [8]. Good adhesion between the layers resulted in extensive interaction between crazes or cracks in the SAN layers and microshear bands in the PC layers. As the number or layers is increased to

*Present address: Rogers Corporation, Rogers, Connecticut 06263, USA
†Present address: Richards Medical Company, Memphis, Tennessee 38116, USA.

0022–2461/90 $03.00 + .12

776, it appears that SAN crazing is significantly suppressed and shear bands are formed in this normally brittle material. This phenomenon is investigated in the present study.

2. Experimental details

Microlayer composites were supplied by The Dow Chemical Company in the form of coextruded sheet. They were approximately 1.20 mm thick with alternating polycarbonate (PC) and styrene–acrylonitrile copolymer (SAN), the outermost layer being PC in all cases. The PC was Merlon (Trademark, Mobay Chemical Company, Pittsburgh, PA) M-40 and the SAN was Tyril (Trademark, The Dow Chemical Company, Midland) 867-B. The SAN composition, 25% by weight acrylonitrile, was chosen for maximum adhesion to PC [9]. Because all the composites were of similar thickness, the thickness of individual layers was varied by using composites with 49, 194, 388 and 776 layers. The PC/SAN volume ratio was kept essentially constant at 65/35 for all the composites except the 388-layer composite, which was about 50/50. Residual orientation in the sheets was determined by annealing 80 mm × 80 mm sheets at 160° C for 1 h under a glass plate and noting the dimensional changes. Extending the annealing time to 2 h had no additional effect.

Tensile specimens were machined from the coextruded sheet both parallel and perpendicular to the coextruded direction according to the ASTM D-638 Type IV geometry. Tests were performed on an Instron testing machine at a strain rate of 54% min^{-1}. The volume change upon necking was measured by extending tensile specimens at a slower strain rate, 0.02% min^{-1}, until a section of neck had formed. With the specimen stressed, the width and thickness were measured and the length change determined from the displacement of markers on the surface of the specimen. Measurements were made on at least 10 specimens of each composite.

Microspecimens about 0.5 mm thick were sectioned from the thickness of the coextruded sheet with a diamond cutter. Both surfaces were polished with 50% aqueous suspensions of first 1 μm and then 0.5 μm aluminium oxide powder from the Buehler Company, Lake Bluff, IL. A guage section was prepared by polishing about one-quarter of the thickness from a small section of the specimen. The microspecimen was mounted in a hand stretcher and slowly extended under an Olympus BH2 polarizing optical microscope. The specimen was photographed from time to time as it was extended. Unless otherwise specified, the results presented are for unannealed specimens tested parallel to the extrusion direction.

3. Results

3.1. Stress-strain behaviour

Typical stress–strain curves of 49, 194, 388 and 776 layer composites tested parallel to the extrusion direction are shown in Fig. 1; all four composites deform in a ductile manner with necking and have approximately the same modulus (2.6 GPa) and yield stress (70 MPa), but the fracture strain increases with

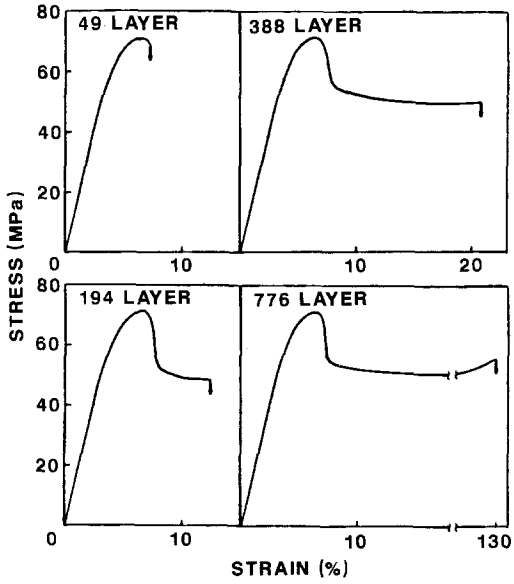

Figure 1 Stress–strain curves of 49-, 194-, 388- and 776-layer composites.

the number of layers. The modulus of the composites follows the rule of mixtures [8]. The yield stress is also higher than that of PC and intermediate between the PC value (62 MPa) and the shear yield stress of polystyrene (82 MPa) which should be similar to that of SAN. This suggests that the SAN layers are load-bearing at the yield point.

Extensive craze formation perpendicular to the tensile direction was observed in 49- and 194-layer composites prior to necking. Near the maximum stress, crazes extended across the entire width of the specimen when a macro-shear band formed at an angle across the width. In the 49-layer composite, fracture followed immediately while in the 194-layer composite, the neck propagated a short distance before fracture occurred at a total elongation of 12%.

No craze formation or stress whitening was observed visually in 388- and 776-layer composites before necking which again occurred by formation of a macro-shear band. Although the 388-layer composite has a slightly higher SAN content than the others, an overall extension to 20% was achieved before fracture, and in the 776-layer composite the neck propagated through the entire gauge length of the specimen. Delamination of the microlayers might be expected because of the difference in ductility of PC and SAN, but none of the four composites studied showed any sign of delamination prior to fracture. Apparently good adhesion between the PC and SAN layers has given the composites structural integrity that can provide efficient stress transfer through the layer structure.

When the strain rate was decreased from 54 to 0.02% min^{-1}, propagation of a neck for a short distance was achieved in the 49-layer composite. With these specimens it was possible to measure the macroscopic draw ratio, L/L_0, the ratio of segment length, L, after necking to the original length, L_0, and the volume change upon necking. The draw ratio in the neck was the same, 2.0, for all the composites as determined by the length change; however, the volume increased by 29.0 ± 4.7% for the 49-layer

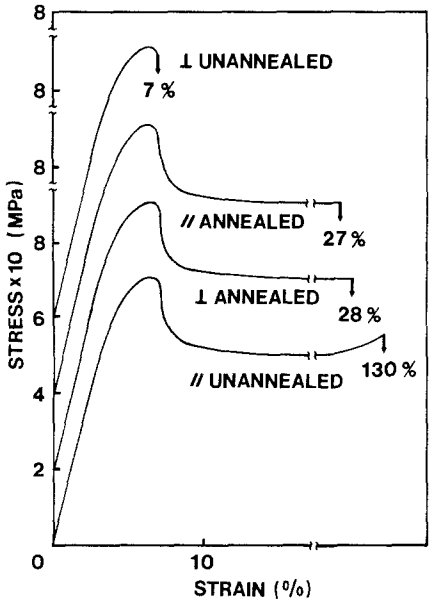

Figure 2 Stress–strain curves of the 776-layer composite tested parallel and perpendicular to the extrusion direction before and after annealing.

composite compared to no significant volume change 0.4 ± 3.7% for the 776-layer composite. Assuming that the cavitational mechanism in the 49-layer composite is crazing and cracking of the SAN layers, the maximum volume increase would be 35% for a draw ratio of 2.0 which is very close to the observation. That there is no volume change in the 776-layer composites suggests that both PC and SAN layers deform by shear yielding, a possibility that is consistent with the absence of visible crazing or other stress whitening in the tensile specimens.

The macroscopic measurements showed no anisotropy in the 49-layer sheets. Within the scatter of the data, the stress–strain relationship was the same whether determined parallel or perpendicular to the extrusion direction. As further confirmation, annealing at 160° C did not produce any dimensional or other changes in the stress–strain relationship. Anisotropy in the 776-layer sheet is clearly indicated by differences in the fracture strain in the directions parallel and perpendicular to the extrusion, Fig. 2, although there is no directional dependence of the modulus or yield stress. When the tensile direction is perpendicular to the flow, crazing is observed, but it is less profuse than in the 49- and 194-layer sheets, and fracture occurs immediately after formation of a neck. Relatively small but significant dimensional changes occur when the 776-layer sheet is annealed at 160° C, the length and width decrease by 9.1 ± 1.2% and 1.7 ± 1.0%, respectively, and the thickness increases by 10.1 ± 2.0%. Annealing removes the anisotropy in the stress–strain behaviour and results in behaviour that is intermediate to that in the two directions before annealing (Fig. 2). The stress–strain curves are identical in the two directions after heat treatment with an elongation at fracture in both directions of about 30%. Some crazing is observed in both directions after annealing but significantly less than in the perpendicular direction before annealing.

3.2. Irreversible deformation mechanisms

The following discussion of the irreversible deformation mechanisms of the four composites is based on the series of micrographs obtained during tensile deformation of microspecimens where micrographs of each composite show the same location on the microspecimen as deformation proceeds. The major features of the microdeformation of the 49-layer composite (Fig. 3) have been previously described by Gregory *et al.* [8]. The first observable event is SAN crazing or cracking initiated at the interface (Fig. 3a). The crazes or cracks grow across the SAN layer until they reach the other interface. With increasing strain, numerous secondary crazes appear in the SAN layers while localized shear deformation in the PC layers is initiated at the interface from the primary SAN crazes (Fig. 3b). The shear zones grow into the PC layer at an angle of 40° to the axis perpendicular to the stress. The shear zones do not initially extend across the entire width of the PC layers, only at higher strains do shear zones initiated from opposite sides of the PC layer coalesce to form bands that extend across the PC layer. During yielding (Fig. 3c), SAN crazes open up into cracks as profuse shear banding produces drawing of the PC layers. In the necked region of the microspecimen (Fig. 3d), the width of the PC layers has decreased about 25% and the shear bands are no longer evident indicating that the PC layers are uniformly extended. The SAN layers show no width reduction but the voids have opened further. When the voids in the SAN layers are about 10 μm long, wedge-shaped notches grow into the PC layers. These notches eventually lead to tearing and fracture of the PC layers. This tearing mechanism is probably responsible for fracture in the neck of the 49-layer composite.

Virtually the same microdeformation behaviour is observed in the 194-layer composite. A microspecimen is shown in Fig. 4 before and after it has necked. Just before necking, Fig. 4a, numerous primary and secondary crazes that have formed in the SAN layers become the sites of shear-band initiation in the PC layers. After necking, Fig. 4b, cracks in the SAN have opened up to form numerous holes while the PC layers are uniformly extended.

The first observable microdeformation event in the 388-layer composite is also cracking or crazing (Fig. 5a), but in this case the deformation sometimes extends across several layers and incorporates one or more PC layers. Shear deformation of PC initiates at a slightly higher strain from the craze or crack tips (Fig. 5b). Up to this point, microdeformation of all the composites follows the same sequence with formation of crazes or cracks in the SAN layers from which shear bands are initiated in the PC layers. The manner in which the 388 layer composite subsequently yields and draws is, however, quite different. A view of the necked region (Fig. 5c) shows that cracks do not open up into voids; instead, the regions between cracks or crazes in SAN layers extend uniformly.

Details of the necking region are shown at higher magnification in Fig. 6. The neck propagates from left to right in the micrographs so that the region on the right-hand side of Fig. 6a has not started to neck. The

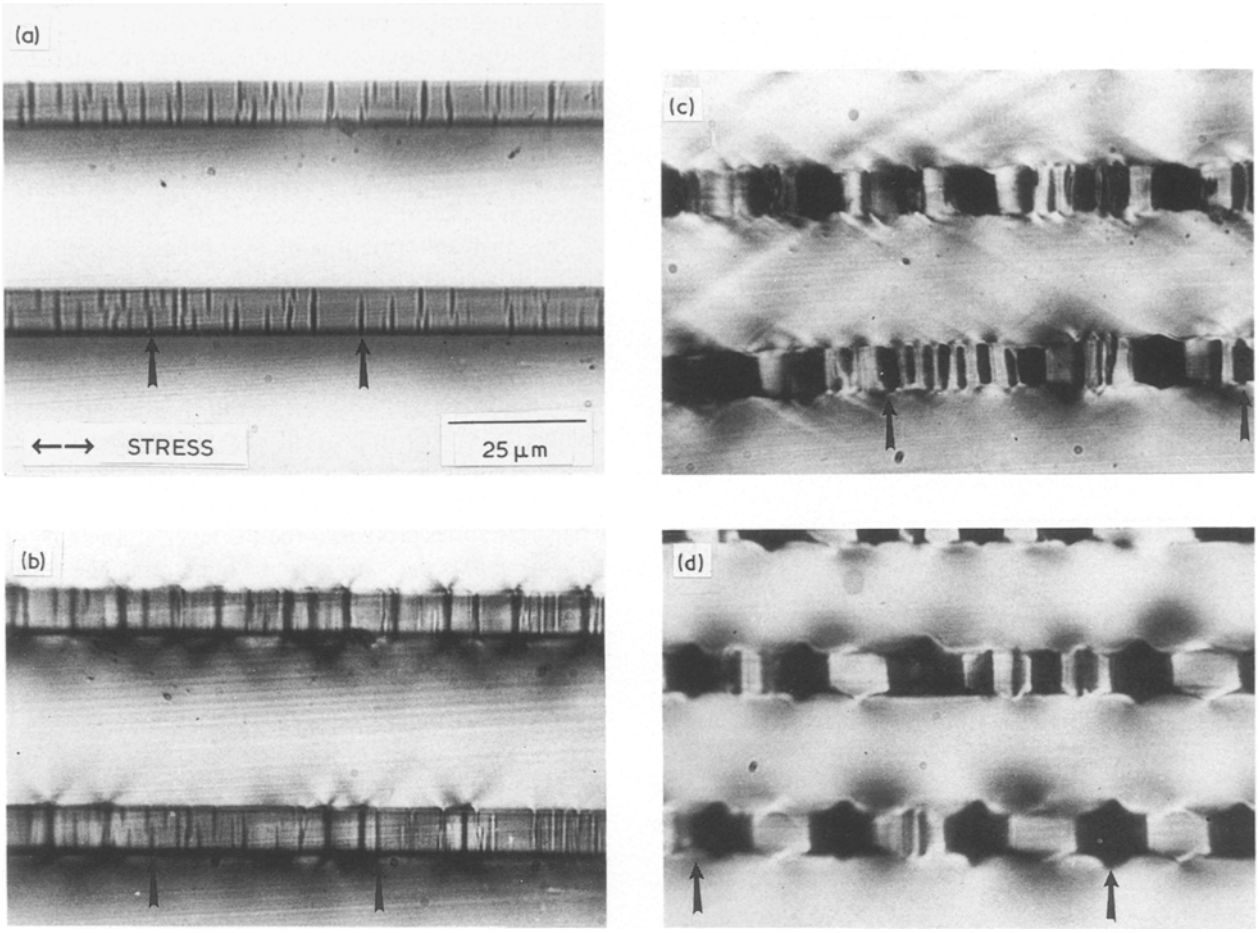

Figure 3 Optical micrographs showing microdeformation of the 49-layer composite: (a) to (d) with increasing strain. The arrows on each micrograph mark the same region of the specimen.

numbers 1 and 2 indicate crazes or cracks that have formed in an SAN layer; shear deformation emanating from the tips into the adjacent PC layers is apparent. The same two crazes or cracks are indicated again in Fig. 6b closer to the neck. The shear bands that in the first micrograph only involve the adjacent PC layer now extend through succeeding SAN and PC layers until they intersect or combine with other similar shear bands to form a network. The number 3 indicates a crack or craze that includes several layers. This is also a site for initiation of shear bands that extend through a number of alternating PC and SAN layers. The cracks or crazes that extend through layers do not open up into voids during necking. Fig. 7 shows one such structure after necking, the SAN layers have broken but the unbroken PC layers in the composite crack prevent it from opening up into a void.

Deformation of the 776-layer composite occurs in a similar manner as described for 388 layers. Numerous cracks or crazes are observed in the SAN but again these do not open up into voids during necking, instead the regions between cracks extend uniformly.

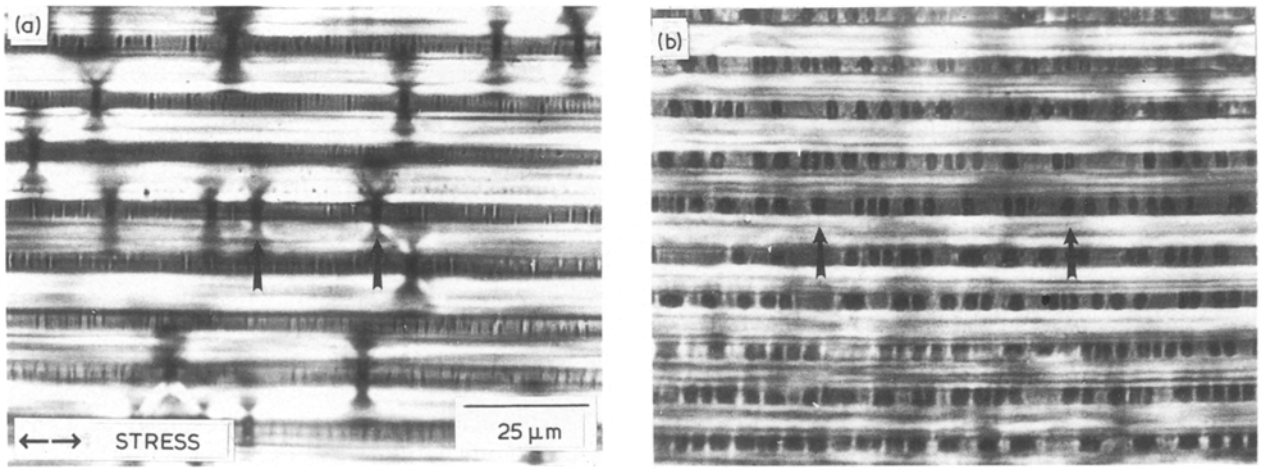

Figure 4 Optical micrographs showing microdeformation of the 194-layer composite: (a) before necking, and (b) after necking.

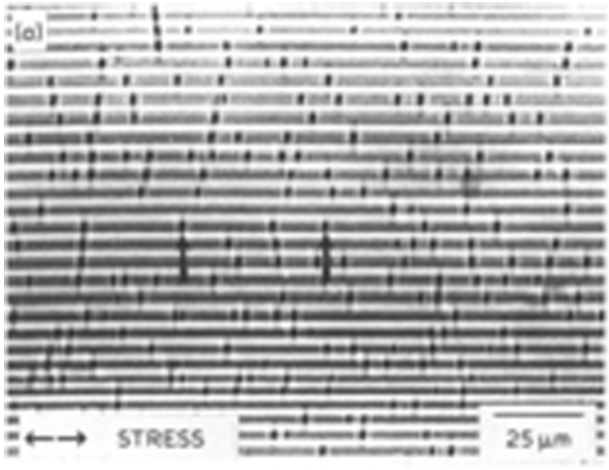

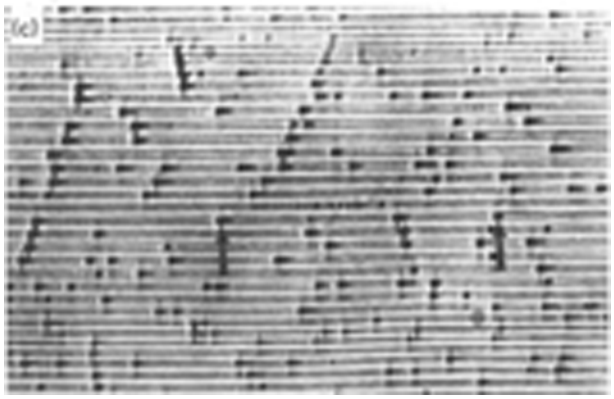

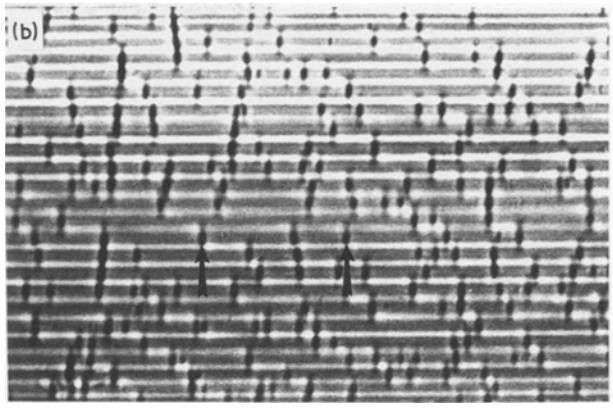

Figure 5 Optical micrographs showing microdeformation of the 388-layer composite: (a) to (c) with increasing strain.

Anisotropy detected in the bulk stress–strain relationship was not reflected in the microdeformation of 776-layer composites, and microspecimens tested perpendicular to the extrusion direction as well as annealed specimens all deformed in the manner described above. Fig. 8 shows an annealed specimen tested parallel to the extrusion direction. The appearance before and after necking again shows that the cracks or crazes do not open up during necking, instead the SAN is uniformly drawn out along with the PC.

The draw ratios of the four composites obtained from tensile measurements and from displacement markers on the microspecimens are compared in Table I. Both methods give values of about 2.0 for all the composites. The draw ratio of individual SAN layers was obtained by comparing the lengths of void areas to SAN areas in micrographs of the neck. The draw ratio, λ, of SAN is then given by

$$\lambda_{SAN} = 2.0\left(1 + \frac{l_{void}}{l_{SAN}}\right)^{-1} \quad (1)$$

where l_{SAN} and l_{void} are the total lengths of the SAN segments and the voided regions, respectively, of a SAN layer in the neck. A draw ratio of 1.0 means the SAN layers fracture in a brittle manner as is the case for the 49- and 194-layer composites, Table I. Larger values up to a maximum of 2.0 reflect the extent to which the SAN has drawn. The values given in Table I for the 388- and 776-layer composites are significantly larger than 1.0 indicating that SAN has shear yielded.

TABLE I Draw ratio of microlayer composites

Composite (layers)	Layer thickness PC/SAN (μm)	Draw ratio		λ_{SAN} (Eq. 1)
		Bulk	Micro	
49	30/18	2.0	2.0	1.05
194	8/5	2.0	1.9	1.02
388	3/3	2.0	2.0	1.54
776	2/1	2.0	2.1	1.82

4. Discussion

In seeking to understand the effects of layer thickness on macroscopic properties such as toughness and elongation at fracture, it is appropriate to develop correlations with the microdeformation mechanisms which occur at the size scale of the layer thickness. The two types of microdeformation behaviour observed in PC/SAN composites, that which characterizes the 49- and 194-layer composites and that of the more ductile 388- and 776-layer composites, are shown schematically in Fig. 9. In all cases, the initial microdeformation event is craze or crack formation in the SAN layers initiated at the interface. At somewhat higher stresses the primary crazes initiate shear deformation in PC layers. In the 49- and 194-layer composites these shear bands extends only part way into the PC layer (Fig. 9); shear bands span the PC layer only as the yield stress is approached and bands from opposite sides coalesce. In these composites individual layers exhibit behaviour that is characteristic of the bulk, that is, SAN layers craze or crack while PC layers undergo shear deformation. Constraints imposed by the microlayer geometry cause shear deformation in the PC to initiate at stress concentrations at the interface caused by SAN crazing or cracking, but do not produce any change in the mechanisms of tensile deformation. Deformation of the 388- and 776-layer composites also begins with crazing or cracking of SAN layers but in this case shear bands that initiate from the crack tips extend through both PC and SAN layers (Fig. 9b). When yielding occurs, SAN layers are drawn along with the PC in a ductile manner. In these composites, the layered morphology has resulted in a change in deformation mechanisms of SAN from brittle fracture to shear yielding.

In microlayer composites, SAN layers undergo

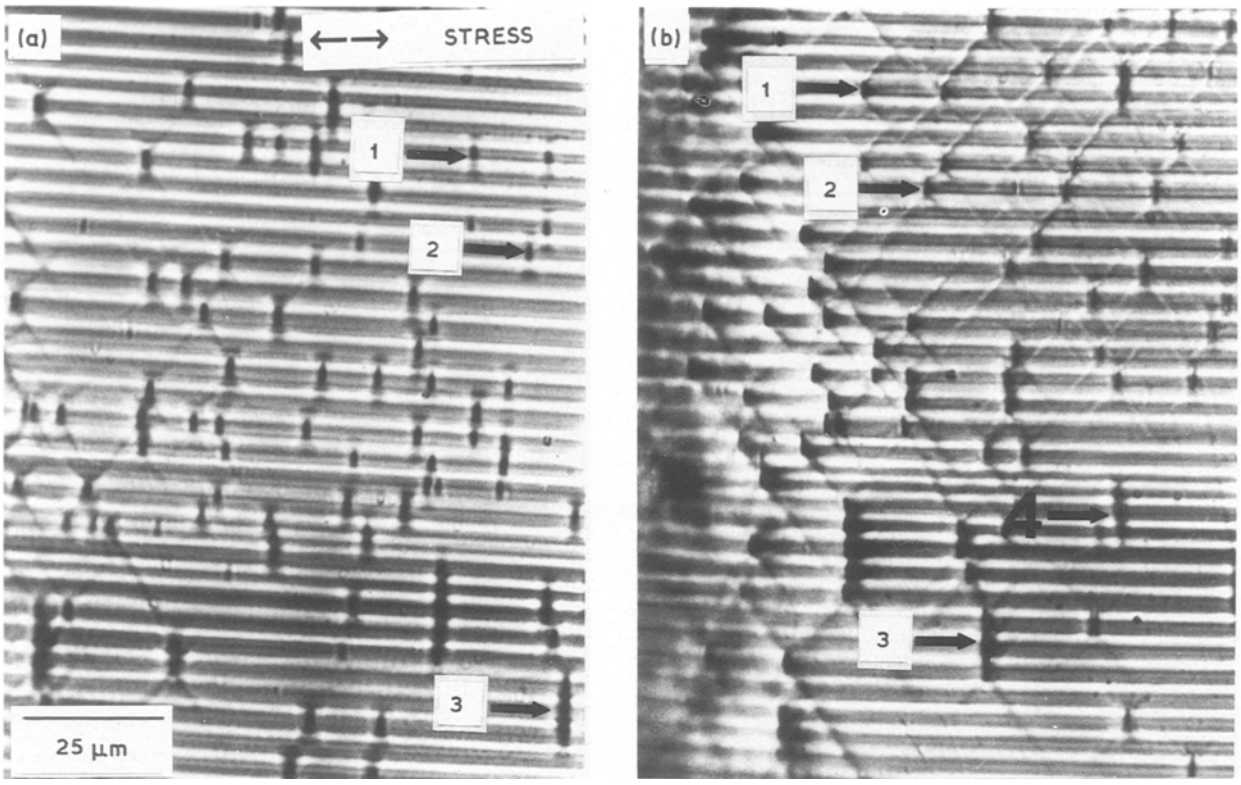

Figure 6 Detail of the necking region of the 388-layer composite (a) and (b) show progression of the neck from left to right.

crazing easily at interfacial defects which act as stress concentrators. With increasing load, the SAN crazes open up into cracks which are subsequently arrested by the neighbouring ductile PC layers. The SAN crack does not grow further by tearing the neighbouring PC layers, but creates a minute depression at the interface into the adjacent PC layer. Thus the numerous SAN cracks lead to the formation of many micronotches in the PC layers.

In pure polycarbonate, the shear yielding modes under slow tensile loading in a semicircular notched specimen are characterized by core yielding, hinge shear and intersecting shear [10]. In the nearly plane strain condition, the dominating shear mode is hinge shear; whereas in the nearly plane stress condition, the dominating shear mode is intersecting shear. It is also true that with increasing stress, the occurrence of the shear modes is in the sequence of core yielding, hinge shear and eventually intersecting shear.

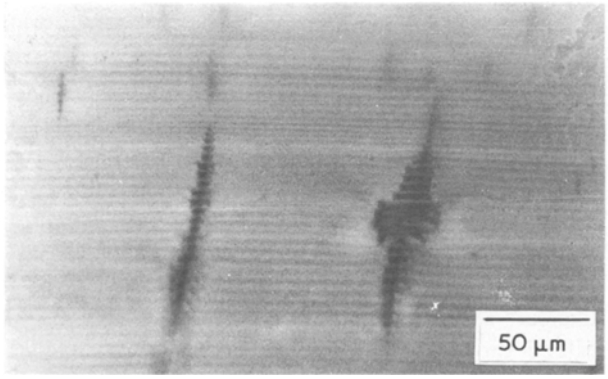

Figure 7 Optical micrograph showing composite cracks in a necked region of the 388-layer composite.

The shear deformation that initiates from the craze tip into the PC layer of the microlayer composites is very similar to, if not identical to, hinge shear in PC. It is also reasonable to assume that the micronotches in the PC layers are close to semicircular due to the fact that shear deformation grows at the same angle 40° as the hinge shear in semicircularly notched PC. It should be pointed out that in all the microlayer composites, the core yielding zone would be too small to be observed at this resolution. On the other hand, because the microspecimen thickness, about 0.5 mm, is much greater than the individual layer width, it is reasonable to assume that the plane strain condition exists at the tip of the micronotch. Hence the dominance of hinge shear from the micronotch tip is the expected mode of localized shear yielding before macroscopic necking occurs.

It appears that growth of hinge shear from a micronotch in the PC layer influences the failure behaviour of the adjacent SAN layer. Following the previous study [10], the hinge shear length is given by

$$\frac{L_h}{a} = \frac{1}{2}\left[\sec\left(\frac{\pi\sigma}{2\sigma_{ys}}\right) - 1\right] \quad (2)$$

where L_h and a represent the hinge length and notch length, σ and σ_{ys} represent the tensile stress and the yield stress of PC. The dimension of the micronotch is taken as the length of the depression into the PC layer, estimated from the micrographs to be 0.75 μm for all the composites. The length of the hinge shear band

Figure 8 Optical micrographs showing microdeformation of the annealed 776-layer composite deformed parallel to the extrusion direction: the same region is shown (a) before necking, and (b) after necking.

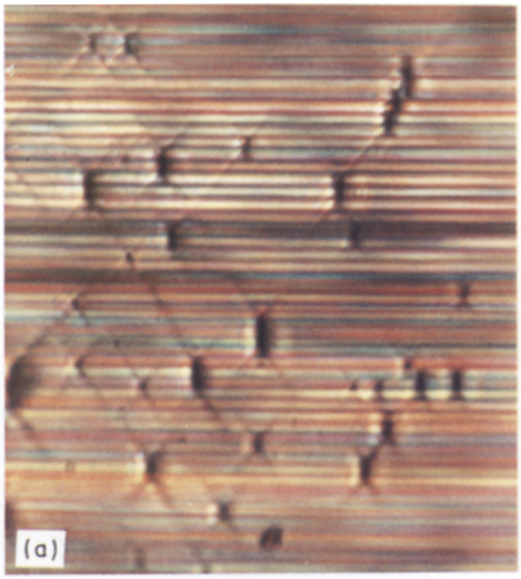
(a)

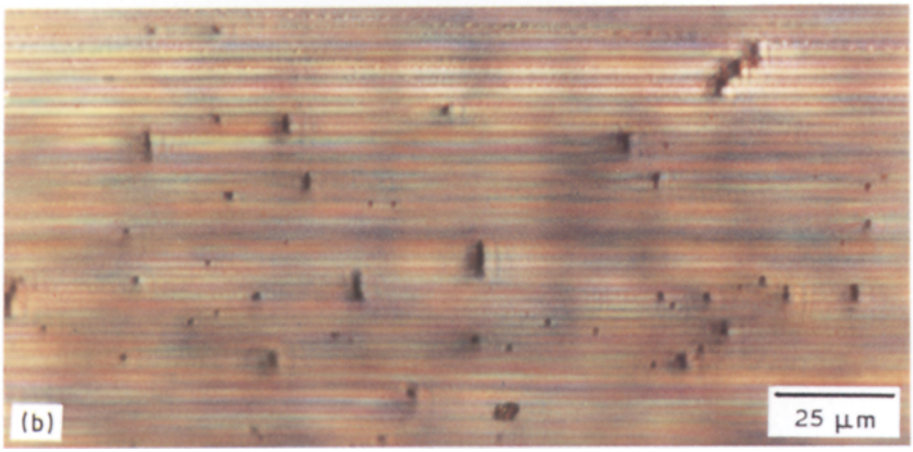
(b)
25 μm

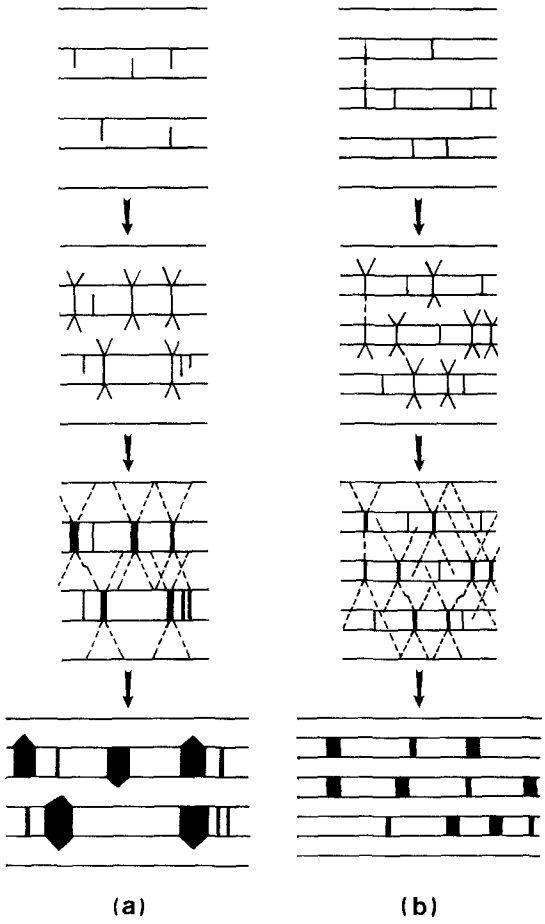

Figure 9 Schematic representation showing microdeformation in the microlayer composites with increasing strain: (a) 49- and 194-layer composites, and (b) 388- and 776-layer composites.

calculated from Equation 2, shown in Fig. 10 for three values of the tensile stress, gives excellent correlation with actual shear band lengths observed in micrographs taken close to the yield point of the PC layers. Shear bands in Fig. 3b, a micrograph of the 49-layer composite, extend about a quarter of the way into the PC layer; at a similar position, Fig. 4a, shear bands in the 194-layer composite extend most of the way across the PC layer but do not reach the next SAN layer. This is precisely what the calculation suggests for a stress in the PC layers close to the 98% of the yield stress, Figs 10a and b. On the other hand, where the shear bands do not intersect or coalesce with other shear bands, they extend through the PC layer and the next SAN layer into the succeeding PC layer in the 388-layer composite, Fig. 6, and may extend through many layers in the 766-layer composite, Fig. 8a. This is consistent with the calculation, Figs 10c and d.

As indicated in Fig. 10, when the stress on the PC layer approaches 98% of the yield stress the hinge shear band has not grown far enough in the 49- and 194-layer composites to reach the interface with the next SAN layer. In these composites, shear bands that span the PC layer form by connection of hinge shear bands emanating from crazes or cracks on opposite sides of the PC layer. During macroscopic necking, localized extension of individual PC layers propagates from these shear bands. Because good interfacial adhesion prevents delamination, extension of the PC layer enlarges the SAN crack to produce a hole. The

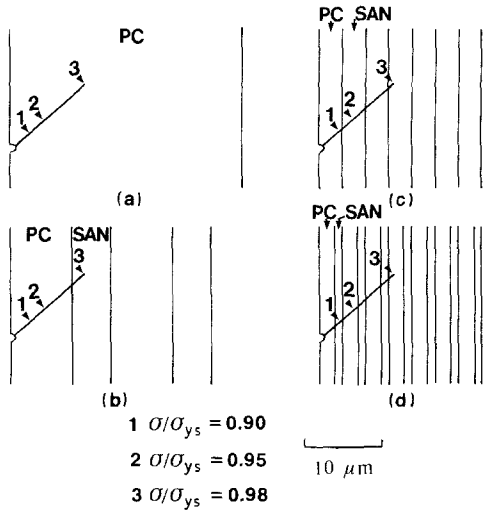

Figure 10 Hinge shear length at 90%, 95% and 98% of the PC yield stress calculated from Equation 2: (a) 49-layer composite, (b) 194-layer composite, (c) 388-layer composite, and (d) 776-layer composite. The drawings are to scale.

effects of interfacial constraints on the local shear displacement of PC also cause the wedge-shaped notches that initiate catastrophic fracture.

In contrast, at 98% of the yield stress the calculated hinge shear length in the 388- and 776-layer composites extends through the PC layer and further into adjacent SAN and PC layers. For SAN alone in simple tension, the craze initiation stress is lower than the shear band initiation stress. Therefore, the dilational mechanism would normally precede the shear mechanism. However, impingement of the PC shear band is expected to change the stress state of SAN near that point. Changes in stress state are known to alter the deformation mechanism of PS [11] from crazing to shearing, and furthermore it is known that the local stress state plays a more critical role than the remote stress field.

5. Conclusions

This investigation of the effects of layer thickness on the deformation behaviour of microlayer composites with alternating PC and SAN layers led to the following conclusions.

1. Composites with 49, 194, 388 and 776 layers all yield in uniaxial tension with the same yield stress, but the fracture strain, which represents how far the neck propagates, increases with the number of layers. The absence of visible crazing or significant volume change during necking of the 388 and 776 layer composites indicates that in these instances crazing is suppressed.

2. A transition in the microdeformation behaviour is observed as the layer thickness decreases. In the 49- and 194-layer composites individual layers exhibit behaviour that is characteristic of the bulk. As the number of layers is increased to 388 and 776, SAN crazing and cracking is suppressed while shear bands form that extend through several layers.

3. Shear deformation of the SAN is attributed to the local shear stress concentration at the interface created by impingement of a PC shear band. The effect of layer thickness is consistent with calculations of shear band length from the literature.

Acknowledgements

This research was generously supported by The Dow Chemical Company and the National Science Foundation (DMR87-13041).

References

1. W. J. SHRENK, US Pat. 3 884 606 (1975).
2. W. J. SHRENK and T. ALFREY Jr, in "Polymer Blends", Vol. 1, edited by D. R. Paul and S. Newman (Academic, New York, 1978) Ch. 15, p. 129.
3. W. J. SHRENK, D. S. CHISHOLM, K. J. CLEEREMAN and T. ALFREY Jr., US Pat. 3 576 707 (1971).
4. J. A. RADFORD, T. ALFREY Jr and W. J. SHRENK, *Polym. Engng. Sci.* **13** (1973) 216.
5. T. ALFREY Jr and W. J. SHRENK, US Pat. 3 711 176 (1973).
6. W. J. SHRENK and T. ALFREY Jr, *Polym. Engng. Sci.* **9** (1969) 393.
7. J. IM and A. HILTNER, Microlayer Composites in "High Performance Polymers", edited by E. Baer and A. Moet (Hanser International, Munich, 1990).
8. B. L. GREGORY, A. SIEGMANN, J. IM, A. HILTNER and E. BAER, *J. Mater. Sci.* **22** (1987) 532.
9. J. D. KEITZ, J. W. BARLOW and D. R. PAUL, *Appl. Polym. Sci.* **29** (1984) 3131.
10. M. MA, K. VIJAYAN, J. IM, A. HILTNER and E. BAER, *J. Mater. Sci.* **24** (1989) 2687.
11. K. MATSUSHIGE, S. V. RADCLIFFE and E. BAER, *ibid.* **10** (1975) 833.

Received 15 December 1988
and accepted 23 August 1989